ARCHIVIO ISTITUZIONALE DELLA RICERCA

Alma Mater Studiorum Università di Bologna
Archivio istituzionale della ricerca

Preclinical Pharmacokinetics in Tumors and Normal Tissues of the Antigene PNA Oligonucleotide MYCN-Inhibitor BGA002

This is the final peer-reviewed author's accepted manuscript (postprint) of the following publication:

Published Version:
Scardovi, A.L., Bartolucci, D., Montemurro, L., Bortolotti, S., Angelucci, S., Amadesi, C., et al. (2024). Preclinical Pharmacokinetics in Tumors and Normal Tissues of the Antigene PNA Oligonucleotide MYCN-Inhibitor BGA002. NUCLEIC ACID THERAPEUTICS, 34(4), 173-187 [10.1089/nat.2024.0005].

Availability:
This version is available at: https://hdl.handle.net/11585/983179 since: 2024-09-12

Published:

DOI: http://doi.org/10.1089/nat.2024.0005

Terms of use:

Some rights reserved. The terms and conditions for the reuse of this version of the manuscript are specified in the publishing policy. For all terms of use and more information see the publisher's website.

This item was downloaded from IRIS Università di Bologna (https://cris.unibo.it/).
When citing, please refer to the published version.

(Article begins on next page)

19 July 2026

Manuscript (including text, tables and captions)

Click here to view linked References

Click here to access/download;Manuscript (including text, tables and captions);Preclinical pharmacokinetics in tumors

Preclinical pharmacokinetics in tumors and normal tissues of the antigene PNA oligonucleotide MYCN-inhibitor BGA002

AUTHORS

Anna Lisa Scardovi[1], Damiano Bartolucci[1*], Luca Montemurro[2], Sonia Bortolotti[1], Silvia Angelucci[1], Camilla Amadesi[1], Giammario Nieddu[1], Sean Oosterholt[3], Lucia Cerisoli[1], Oscar Della Pasqua[3], Andrea Pession[4], Patrizia Hrelia[5], Roberto Tonelli[5**]*

AFFILIATION

[1]R&D Department, BIOGENERA SpA, Bologna, Italy.

[2] AGEOP Ricerca OdV, IRCCS S.Orsola Hospital, Pediatric Oncology and Hematology Unit, Bologna, Italy

[3]Clinical Pharmacology & Therapeutics Group, University College London, London, United Kingdom.

[4]University Hospital of Bologna, IRCCS, Pediatric Unit, Bologna, Italy.

[5]Department of Pharmacy and Biotechnologies, University of Bologna, Bologna, Italy.

*Anna Lisa Scardovi and Damiano Bartolucci equally contributed to this work.

**Corresponding author: Roberto.tonelli@unibo.it

ABSTRACT

Although MYCN has been considered an undruggable target, MYCN alterations confer poor prognosis in many pediatric and adult cancers. The novel MYCN-specific inhibitor BGA002 is an antigene PNA oligonucleotide covalently bound to a nuclear-localization-signal peptide.

In the present study, we characterized the pharmacokinetics of BGA002 by the setting-up of a novel specific ELISA assay. After single and repeated administration to mice, BGA002 concentrations in plasma showed linear pharmacokinetics, with dose proportional increase across the tested dose lev-

els, and similar exposure between male and female, and between intravenous and subcutaneous route of administration. Repeated dosing resulted in no accumulation in plasma. Biodistribution up to seven days after single subcutaneous administration of [^{14}C]-radiolabeled BGA002, showed broad tissues and organ distribution (suggesting a potential capability to reach primary tumor and metastasis in several body sites), with high concentrations in kidney, liver, spleen, lymph nodes, adrenals, and bone marrow.

Remarkably, we demonstrated that BGA002 concentrates in tumors after repeated systemic administrations in three mouse models with MYCN-amplification (neuroblastoma, rhabdomyosarcoma and small-cell-lung-cancer), leading to a significant reduction in tumor weight. Taking into account the available safety profile of BGA002, these data support further evaluation of BGA002 in patients with MYCN-positive tumors.

INTRODUCTION

MYCN is a member of the MYC family of oncogenes, and is an oncogenic driver in many types of cancers[1]. Deregulation of MYCN occurs in both pediatric and adult cancers. MYCN-amplification (MNA) and/or overexpression have been found in pediatric cancers including neuroblastoma (NB), rhabdomyosarcoma (RMS), medulloblastoma, Wilms tumor and retinoblastoma. In particular, NB is one of the deadliest cancers that occur in early childhood and represents 7% of pediatric malignancies[1–3]. About 25% of patients with NB present MNA which is linked to a poor prognosis, metastasis, and advanced stage disease[1–3]. RMS is the most common pediatric soft tissue sarcoma, and a major cause of cancer death in children. MNA is present in about 25% of cases and MYCN overexpression occurs in 55%. It is associated with adverse prognosis and is a feature of the more aggressive alveolar subtype (ARMS)[4]. Similarly, MNA is also present in adult cancers, and occurs in small cell lung cancers (SCLC)[1] (15-20%)[5,6], in neuroendocrine prostate cancers (40%), in prostate adenocarcinomas (5%)[7], and in basal cell carcinomas (17.5%)[1], while overexpression of MYCN is present in a subset of T-cell acute lymphoblastic leukemias, glioblastoma multiforme and breast cancer[1]. Importantly, the amplification or overexpression of MYCN in the majority of these adult cancers is associated with a poor prognosis[1]. Normally, MYCN expression is restricted during embryogenesis and has a very limited pattern of expression in normal cells after birth[8]. Given its crucial role in MYCN-positive tumors, one should consider this as a promising target[1]. However, N-Myc protein is deemed an undruggable target and drug discovery approaches aimed at blocking N-Myc protein have largely failed[9]. While indirect strategies have been proposed, none of these has proven to be effective in standard clinical practice [1,3,10].

We have previously demonstrated that an alternative approach consists in the specific gene expression inhibition at the level of chromosomal DNA through MYCN-specific antigene peptide nucleic acid (PNA) oligonucleotide covalently linked to a nuclear localization signal (NLS) peptide[2,4,11–14]. The antigene oligonucleotide approach (via persistent and specific block at the level of the target gene transcription) has shown advantages compared to the block of mRNA translation by antisense

PNA oligonucleotide strategies[2,4,11–15]. In particular, BGA002 is a MYCN specific antigene PNA that inhibits MYCN gene expression, yielding a potent and specific anti-tumor activity both *in vitro* and *in vivo*[2,13,14]. PNAs are oligonucleotide mimetics, in which the anionic sugar-phosphate backbone of the nucleic acids is replaced with an achiral, uncharged polyamide backbone[16]. PNAs showed promising results in diagnostic or therapeutic applications as antisense or antigene drugs, due to their extraordinary stability against enzymatic degradation by proteases and nucleases and their ability to potently and specifically bind with high affinity their target complementary sequences in DNA or RNA[2,4,11,15]. PNAs have distinctive characteristics, which allow them to be used for antigene application because their neutral backbone avoids the electrostatic repulsion normally encountered between the negatively charged double strand DNA[2,4,11,17]. PNAs are amenable to manipulations more than other nucleic acid analogues, and a straightforward approach to improve its pharmacological properties lies in the conjugation of PNA to short synthetic carrier peptides[18,19]. Different type of peptides have been evaluated[2,4,11,18,20–25], with the aim to improve the limited solubility, low cellular uptake, poor biodistribution and rapid excretion of naked PNA oligonucleotides[26], which has prevented their broad application as oligonucleotide therapeutics.

In an attempt to explore the pharmacokinetic-pharmacodynamic relationship of BGA002, and predict the exposure required for anti-tumor activity in humans, as well as establish the dosing requirements for a first-time-in-human study, we investigated the pharmacokinetics (PK) and pharmacodynamics (PD) profiles in pediatric and adult MYCN-positive tumor mouse models after single and repeated systemic administration of BGA002. The characterization of the pharmacokinetics in plasma was complemented by the evaluation of the biodistribution in healthy tissues, organs, and blood, taking into accounts the potential effect of route of administration, sex, and accumulation. In addition, to overcome the lack of a standardized methodology, here we report the development and application of a novel hybridization-based ELISA approach for the quantification of the MYCN-inhibitor BGA002 PNA-peptide in biofluids, as well as in murine tissues and tumors. We anticipate that, together with information on the safety profile of BGA002, these results provide the basis for

the design of oligonucleotide-based cancer therapeutics in a prospective first-time-in-human study. Characterization of the pharmacokinetics and pharmacodynamics of BGA002 may also give a benchmark for the development of other PNA-peptide inhibitors.

RESULTS

Pharmacokinetics of BGA002 in mice.

The pharmacokinetic profile after single and repeated administration of BGA002 to mice was evaluated with a new specific hybridization-based ELISA assay of plasma. The concentration vs. time profiles were comparable after single dose and after 28 days of repeated SC administration, as demonstrated by both C_{max} and $AUC_{(0-t)}$ values. Absorption following SC administration was fast, with T_{max} being achieved after 10 min. Systemic exposure was similar between male and female, irrespective of the dose level, with comparable exposure between intravenous (IV) and subcutaneous (SC) route of administrations (Figure 1 a, b, c, S1, S2 and S3). BGA002 was quantifiable up to eight hours in plasma (Figure 1 a, b and c, Supplementary Table S1 and S2), after which drug levels were below the limited of detection. There was no accumulation after repeated dosing (daily for 28 days) (Figure 1 d, Supplementary Table S3). In addition, exposure increased in a dose-proportional manner, despite interindividual variability (Figure 1 e, Supplementary Table S3). The $AUC_{(0-t)}$ after single SC administration of 2.5, 7.5 and 25 mg/kg dose were 478.1, 1331.1 and 3433.6 h*ng/mL, respectively. No accumulation, metabolic inhibition of induction was observed following repeated dosing, which resulted in similar exposure range (namely, 428.8, 1208.7 and 2801.5 h*ng/mL after 2.5, 7.5 and 25 mg/kg dose, respectively) (Table 1). C_{max} also increased in a dose-dependent manner after SC administration (198, 410, 1031 ng/mL after 2.5, 7.5 and 25 mg/kg dose, respectively). Similar findings were observed between sexes (Table 1).

The elimination half-life ($t_{1/2}$) was short, but quite variable in the different dosing groups, but no significant differences were observed between males and females, for both IV and SC administration (Table 1). Volume of distribution (V_d) values indicate drug distribution beyond total body wa-

ter. Systemic body clearance (Cl_b) estimates showed high clearance, even though results were not affected by induction or inhibition mechanisms (Table 1). The median of relative bioavailability (F) for the subcutaneous route, independently from the dose was calculated as 98.41 in male and 83.67 in female (p-value = 0.6667) (Table 1). PK in rabbits showed a higher (up to ten fold) exposure compared to mice (Supp Fig. S5). Volume of distribution was higher in mice after SC administration (35218.41 mL/kg) than in rabbits after IV infusion (3086.70 mL/kg) at the same dose of 2.5 mg/kg (this could indicate a higher distribution in tissue in mice than in rabbits) (supp Table S5). Clearance was higher in mice after SC administration (3261.74 ml/h/kg) than in rabbits after IV infusion (694.43 ml/h/kg) (this indicates a higher elimination rate in mice compared to rabbits) (supp Table S5).

BGA002 has a broad biodistribution in organs and tissues in mice

In order to examine the tissue biodistribution of BGA002 after single subcutaneous administration, radioactive BGA002 containing a [^{14}C]-acetylated at the C-terminus ([^{14}C]-Ac-BGA002) was injected into male and female CD-1 mice at a target dose of 15 mg/kg. Total radioactivity in selected tissues was investigated by quantitative whole body autoradiography (QWBA) at several timepoints (1, 4, 8, 24, 48 and 168 h post dose) (Figure S1 and S2). The concentrations of total radioactivity in selected organs and tissues of male CD-1 mice are presented in Figure 2 a and b with a representative example of the autoradiography shown in Figure 2 c. The results indicate a wide distribution of BGA002 into several tissues and organs, with the kidney, liver, spleen, bone marrow, lymph nodes and adrenals (Figure 2 a and b) exposed to the highest levels of radioactivity. The results also confirmed fast clearance from plasma, with the highest concentrations of BGA002 detected at the first sampling time point (i.e., 1 h post dose, 1.20 µg equiv/g) and less than half the quantity at 4 h post dose, with further decrease in the subsequent time points. The majority of the tissues showed high concentration between 4-24 h post dose, but it was not possible to identify a clear T_{max}. In both sexes, diffusion and biodistribution from the dose injection site was very slow, with

radioactivity still visible at the injection site and in the surrounding areas at 168 h post dose (last time point) (Figure 2 a and b). Radioactivity remained well above the limit of detection in most tissues at this time point. The elimination half-life could not be estimated due to the high level of radioactivity still present at the last time point. Concentrations of radioactivity in the spinal cord and brain in both male and female animals were low, indicating limited penetration through the blood-brain barrier (Figure 2 a, b and c).

BGA002 highly concentrates in tumors and correlates with efficacy in different xenograft mouse models

The pharmacokinetic (PK) profile of BGA002 in tumors was investigated in three tumor xenograft mouse models with MNA and MYCN-expression (NB, RMS and SCLC). BGA002 was administered subcutaneously (SC) for 15 days (15 mg/kg/day for RMS and 10 mg/kg/day for NB) or 9 days (5 mg/kg/day; 15 mg/kg/day for SCLC), and its concentration in the tumor was compared with the liver (a healthy organ showing the highest BGA002 concentration in biodistribution studies). These results reveal that BGA002 penetrated into the tumors in all the three mouse models (Figure 3). In particular, in NB tumors BGA002 reached a concentration 3-fold higher compared to the liver in the same animals. The anti-tumor activity of BGA002 was evaluated *in vivo* in the same three xenograft murine models. In the RMS model, treatment with BGA002 (SC administration of 15 mg/kg/day for 15 days) resulted in tumor weight decrease of more than 70% (p-value = 0.064) (Figure 4 b). In addition, BGA002 (SC administration for 9 days) at 5 and 15 mg/kg/day induced tumor weight decrease of 15% (p= 0.894) and 59% (p=0.032), respectively in the multidrug resistant SCLC mouse model (Figure 4 b). Similarly, significant reduction of the N-Myc protein (evaluated by Western blot) was observed in the RMS model and multidrug resistant SCLC mouse model (Figure 4 a and c). Moreover, a similar pattern of response was observed in a histological analysis of tumor vascularization, leading to tumor vessels elimination after treatment at 15 mg/kg/day (Figure S4). Finally, we previously reported the *in vivo* efficacy of BGA002 in a MNA-NB murine model[2], where we

found that SC administration for 15 days of 2.5, 5 or 10 mg/kg/day resulted in a potent dose – response tumor growth inhibition, that reached tumor elimination after treatment with 10 mg/kg/day. In this MNA-NB mouse model, treatment with BGA002 at 5 mg/kg/day yielded a consistent reduction of the N-Myc protein (evaluated by IHC) and of the tumor vessels[2].

DISCUSSION

It is well established that MYCN is a key oncogenic driver in many types of pediatric and adult cancers[1]. MYCN drives cancer cells towards a stem-like phenotype that affects many different processes, including induction of proliferation, cell growth, immune escape, invasion, metastases, alteration of metabolism, and inhibition of apoptosis[1]. In particular, MNA and/or overexpression is a key feature of highly aggressive and deadliest cancer subtypes, and the majority of these tumors is associated with a poor prognosis[1]. Considering the differences in the pattern of expression in normal cells and its role in MYCN-positive tumors, MYCN can be considered tumor-specific and a promising target for therapeutic interventions[8]. We have previously reported an alternative approach based on a selective MYCN gene expression inhibition at the level of chromosomal DNA, through a potent specific antigene PNA oligonucleotide named BGA002[2,4,11–14]. The BGA002 sequence is complementary to a sequence of MYCN gene in murine and in human genomes, showing uniqueness in the latter. In particular, compared to the first lead anti-MYCN antigene PNA BGA001[4,11,12], BGA002 demonstrated a more potent and specific inhibition of MYCN expression[2,13,14]. BGA002 caused the block of different MYCN-related tumorigenic elements that contribute to cell deregulations, a dose dependent tumor growth inhibition and the induction of apoptosis in MYCN-positive NB and SCLC cells [2,14]; in vivo systemic treatment with BGA002 leads to potent anti-tumor activity in MNA-NB and MNA-SCLC[2,14].

In previous studies, the antigene PNA oligonucleotide approach (via persistent and specific block at the level of the target gene transcription) showed pharmacological advantages compared to the block of mRNA translation by antisense PNA oligonucleotide strategies[2,4,11,15]. PNAs have unique

characteristics for antigene application, as their neutral backbone avoids the electrostatic repulsion normally encountered between the negatively charged double strand DNA. However, naked PNA oligonucleotides showed limited solubility, low cellular uptake, poor biodistribution, tend to exhibit low plasma protein binding and are rapidly excreted in the urine[26,27], that prevented their broad application as therapeutics. Because PNA oligonucleotides have a peptide backbone, the most straightforward approach to overcome these limitations and improve its physicochemical and biological properties is the conjugation of PNA to short synthetic carrier peptides. Different types of peptides have been evaluated, that conferred improved pharmacological properties, ranging from cell penetrating peptides focused to optimize the cellular delivery, to peptides that showed improvement to the PK and biodistribution[18,19].

Regarding the anti-MYCN BGA002, because of its pharmacological mechanism of action as an antigene PNA oligonucleotide, delivery in the cell nucleus is a key point for selection of an optimal peptide. Therefore, BGA002 contains a covalently linked NLS peptide that we previously selected after experimental evaluation of different peptides. The NLS peptide sequence was previously reported by us for the anti-MYCN antigene PNA BGA001[4,11] and by others for an anti-MYC antigene PNA[20,21]. Unlike other reported NLS peptides linked to antigene PNAs[4,11,20,21], the NLS peptide in BGA002 is made by D amino acids to improve its stability and limit degradation by proteases[2,13,14]. Our previous data showed that BGA002 has an efficient cellular and nuclear accessibility in cancer cells[2]. We previously showed that NLS peptide is important also to improve the pharmacodynamics properties for the target DNA sequence of the MYCN gene[28].

Here we report for the first time the development of a novel specific hybridization-based ELISA approach for the characterization of the PK profile of the MYCN-inhibitor BGA002, and its quantification in mouse and rabbit biofluids, as well as in the organs of healthy mice and tumor xenografts.

PK analysis in plasma after single administration of BGA002 in mice showed dose independent, linear pharmacokinetics across the dose range tested, with no evidence of sex differences between

male and female animals. Results also show good bioavailability, as minor differences were observed between IV and SC route of administration. The concentration range achieved after IV and SC is relevant because it provides evidence that SC administration does not contribute to interindividual variability in exposure. It also supports the use of SC route for further evaluation of efficacy, overcoming potential technical problems of daily IV administrations through tail vein in mice. Moreover, the relatively high biovailability of BGA002 following SC administration also opens the possibility to use SC as a route of BGA002 administration in human clinical studies. This would ensure better adherence to treatment and lower the burden of treatment due to the requirements for IV administration.

The PK tissue biodistribution in mice after single subcutaneous administration of [^{14}C]-Ac-BGA002 at several time-points from 1 h up to 7 days, showed a broad biodistribution in several tissues and organs, with a principal exposure observed in the kidney, liver, spleen, bone marrow, lymph nodes and adrenals. This is in line with previous pharmacokinetic studies[19], which indicated that PNA conjugated to short synthetic peptide carriers were rapidly cleared from circulation and distributed to a variety of tissues, with highest concentration in liver, kidney, spleen, mesenteric lymph nodes and adipose tissue (a very similar set of organs to the one we found for BGA002, except to the adipose tissue which in our study is not one of the main organs where BGA002 accumulates). Overall, these data show that peptide-conjugated PNAs overcome the common issues associated with unmodified PNAs, which include poor biodistribution, and they represent a synthetically feasible approach to improve their physicochemical and biological properties.

The broad biodistribution of BGA002 in several organs and tissues could suggest its potential capability to reach primary tumor and metastasis in several different sites in the body. In this respect, it is relevant that BGA002 localized also in the adrenal medulla (that is a preferential primary site of origin for NB), and in the bone marrow (that is a preferential site of metastasis for NB and SCLC). Moreover, the broad biodistribution of BGA002 to several organs and tissues, suggest a wider con-

sideration that the class of the PNAs oligonucleotides covalently bond to the positively charged NLS peptide could also treat other tumors in many different body sites, and even non-oncological diseases affecting these different body sites.

The low biodistribution of BGA002 in the spinal cord and brain, indicate that the blood-brain barrier limits its access to the central nervous system (CNS), most probably because the NLS delivery peptide is positively charged (contain lysine and arginine amino acids). If required, for therapeutic indications requiring CNS biodistribution, naked PNA oligonucleotides for their neutral characteristics can cross the blood brain barrier and reach the CNS[27].

In the present work, we investigated the PK profiles of BGA002 in different MNA and MYCN-expressing tumors. We selected NB and RMS (as relevant examples for poor prognosis MYCN-positive pediatric tumors), and multidrug resistant SCLC (among the poor prognosis MYCN-positive adult tumors). Remarkably, the tumor PK profile showed that repeated systemic administration of BGA002 resulted in its localization in all the three highly aggressive MNA tumor mouse models, with a remarkable 3-fold higher concentration in NB tumor compared to liver. Moreover, the concentration of BGA002 in tumors was associated to an anti-tumor PD activity in all the three MNA tumors. In particular, among the three tumors, the highest PK concentration found in NB was also associated to the highest anti-tumor activity[2], indicating a correlation of BGA002 PK with efficacy in these tumors. MYCN plays a central role in driving tumor evolution, orchestrating several aggressive oncogenic features. Among them, it is well defined the role of MYCN in neovascularization[29,30]. Therefore, our findings about BGA002 concentration in MYCN-expressing tumor might be also linked by the MYCN role in promoting the neovascularization (and thus accessibility) of the tumors. In this respect, it is relevant that treatment with BGA002 in the multidrug resistant SCLC model led to elimination of tumor vascularization, similarly to our previous findings in NB and SCLC[2,13].

As MNA tumors are characterized by a very high amount of N-Myc protein, high-risk and metastatic conditions, we evaluated a daily treatment schedule in MNA mice model to face this dramatic

scenario. For the same reasons, in human clinical trials we would propose frequent administration, while considering the lower pk in human compared to mice.

Preclinical toxicology studies of repeated administration of BGA002 (4 weeks daily) performed in healthy mice under GLP conditions by using concentrations higher than those reported in the present work, showed that it is well tolerated (data not shown).

BGA002 could be proposed in clinical trials as a monotherapy or in combination with selected anti-cancer drugs. In this context, BGA002 already showed to act in synergy with retinoic acid (RA) in MYCN expressing NB, by overcoming RA resistance and restoring RA efficacy[14].

There are only a limited number of preclinical works describing the PK behaviour of administered oligonucleotides in tumors in vivo, and none evaluating the effect of systemic repeated dose treatment[31–33]. Oligonucleotide therapeutics are emerging as promising anti-cancer precision medicines, especially for the targeting of the large number of undruggable proteins (such as that codified by MYCN) and non-coding RNAs[34]. Our new preclinical findings indicate that the MYCN-specific antigene PNA-peptide BGA002 highly concentrates in aggressive MYCN-related tumors and generates anti-tumor efficacy. Our data reinforce the potential role of oligonucleotides in cancer therapy and pose the basis for the first-in-human clinical trials of BGA002 in these highly aggressive MYCN-positive tumors. BGA002 already obtained orphan drug designation for NB by the Food and Drug Administration (FDA) (orphan register: DRU-2017-6085) and the European Medicines Agency (EMA) (orphan drug application: EMA/OD/020/12), for Soft Tissue Sarcomas (including RMS) by EMA (orphan drug application: EMA/OD/037/16) and for SCLC by FDA (orphan register: DRU-2018-6260).

MATERIALS AND METHODS

Chemicals and dose preparation

Biogenera produced BGA002. PNA-peptide was either available, stored at -20°C, and ready for use, or freshly produced by the chemistry department and delivered after purification and dilution to the biology department for non-GLP studies or to the CROs (GLPLife Test, Wil Research, Aptuit and Selcia) for GLP studies. PNA was designed and prepared according to previously published studies[2,4,11,13,14]. BGA002 was prepared starting from lyophilized BGA002 adding either vehicle 2.5% mannitol, 75 mM acetic acid, 25 mM sodium acetate in sterile water for injections or physiological solution 0,9% NaCl (Fresenius Kabi Italia S.r.l.) to reach the desired concentration (according to declare powder quantification). Solution of BGA002 was quantified through spectrophotometer (λ_{260}=170300 L mol^{-1} cm^{-1}) and adjusted to reach 3 mg/mL, then stored at +°4C. Biogenera synthesized an acetylated form of BGA002. The radio labeled [^{14}C]-Ac-BGA002 (Batch No. 8249DCP006-6, radiochemical purity 99.8%) was supplied synthesized by Selcia Limited (UK) as a solution in acetic acid: sodium acetate: HCl (75 mM: 25 mM: 3.6 mM) with 2.5% mannitol at a concentration of 1.16 MBq/mL (3.35 mg [^{14}C]-Ac-BGA002 /mL). The solution was stored in a fridge set to maintain a temperature of +4°C.

Animals: mice

NOD/SCID CB17 mice for PK analysis in tumor and liver and for efficacy studies were born in the animal facility of the Department of Veterinary Medical Science of the University of Bologna (Italy. All experiments were approved by the Scientific Ethical Committee of Bologna University according to protocol no. 7/73/2012 and authorization 564/2018-PR. Pharmacokinetics plasma analysis was performed in juvenile mice (CD1-Swiss) by Glp Life Test. Aptuit and Farefarma performed respectively ELISA analysis and pharmacokinetics analysis. Biodistribution analysis in mice (CD1-Swiss) was performed by Charles River. Animals were maintained according to each CRO internal standard operating procedures. PK and biodistribution studies in mice were performed under GLP compliance.

In-vivo PK/TK experiments in mouse plasma

The studies were conducted with the support of the following CRO:

- In-vivo phase: Glp Life Test, Via Saliceto 3, 40010 Bentivoglio, Bologna, Italy
- Bioanalysis: Aptuit Verona Srl, Via Alessandro Fleming, 4 - 37135 Verona, Italy
- Pharmacokinetic Analysis: Farefarma Srl, Via Ferrari, 9 - 28045 Invorio, Italy

The animals used for the studies include Swiss mice (CD1) (5 weeks old at start of treatment) from the Charles River Laboratories Italy Srl with a health certificate according to Legislative Decree 24/20142.

The rationale for the dose selection of the single dose PK study in mice was based on feasibility studies performed in Biogenera lab that showed good level of quantification at 15 mg/kg dose in tumor and liver, thus this dose and the 3-fold lower dose 5 mg/kg were selected to obtain data in plasma. Rational for the dose selection of the repeated dose PK studies in mice was based on the above mentioned single dose PK study; since the two tested doses of 5 and 15 mg/kg gave well separated kinetic curves, the following doses were selected for the repeated dose PK/TK study: 2.5, 7.5, and 25 mg/kg/die. For the single dose study, two groups, each of 24 male and 24 female mice, were treated by single intravenous (bolus) injection in caudal vein of 100 µL solution containing BGA002 at the following doses: 5 or 15 mg/kg; another group (control) composed of 4 males and 4 females was treated by intravenous (bolus) injection with 100 µL of vehicle; two additional groups, each of 24 male and 24 female mice, were treated by single subcutaneous injection on the back with 100 µL of solution containing BGA002 at the same doses (5 or 15 mg/kg); and a last group (control) composed of 4 males and 4 females was treated by subcutaneous injection on the back with 100 µL of vehicle. The animals were given a single administration and subsequently were sacrificed at 6 different time points for blood collection (time points IV: 5-15-30-60-240-480 minutes; time points SC: 10-30-60-90-180-480 minutes).

For the repeated dose study, three groups each of 36 female mice were treated by SC injection on the back with BGA002 solutions at 25 mg/kg, 7.5 mg/kg or 2.5 mg/kg at a constant volume of 5

mL/kg/die. The volume of solution administered was calculated weekly using the last mean body weight for group. Eighteen animals per group were treated with a single injection while another eighteen animals per group were treated for 28 days with a once-a-day SC injection; all animals were then sacrificed at six (6) different time-points (10-30-60-90-180-480 minutes) for blood collection.

In both studies, the blood was collected from the cava vein before sacrifice of the animal that was anesthetized by inhalation of a mixture of CO_2/O_2 (70% and 30% respectively). A total of 0.3 mL of whole blood was drawn from each of 3 animals per time point and, due to technical sample limitation in juvenile animals, the samples were pooled in a single tube containing enough lithium-heparin to treat 1 ml of blood volume (APTACA company mod 2400/1). The plasma collected from each tube was frozen at about -20°C at least overnight and shipped on dry ice to the Test Site (Aptuit) for the analyses.

Hybridization-based ELISA in plasma and organs (tumor/liver)

To measure the concentration of BGA002 present in plasma samples and in tumor/liver samples a hybridization-based ELISA assay has been developed and validated. Neutravidin coated plates were incubated with a capture probe, biotin-labeled and partially complements BGA002. After incubation and washing, plasma samples were added to the plate where the complex is immobilized by the neutravidin-biotin-binding. After washing a detection probe, digoxigenin-labeled and complementary to the other part of BGA002, was added. Then a detection solution containing anti-digoxigenin-peroxidase (anti-DIG-POD) was added, making possible visualization by addition of tetramethylbenzidine (TMB) that produces a colored product. The amount of color correlates to the amount of BGA002 present. Plates were washed 3 times with 300 µL 5X SSCT buffer; 100 µL of 0.2 µM Capture probe solution in 5X SSCT buffer is added and incubated at RT for 30 minutes. Plates were washed 3 times with 300 µL 2X SSCT buffer; 100 µL of plasma samples/CS/QC were added and incubated at 37°C for 60 minutes. Plates were washed 4 times with 300 µL 2X SSCT

buffer; 100 µL of 0.2 µM of Detection probe solution in 5X SSCT buffer was added and incubated at RT for 60 minutes. Plates were washed 3 times with 300 µL 2X SSCT buffer and 3 times with 300 µL of purified water; 100 µL of Anti-DIGPOD Fab fragments (1:8000) in PBST and incubated at RT for 60 minutes. Plates were washed 3 times with 300 µL 2X SSCT buffer; 100 µL of substrate solution (1-step Ultra TMB ELISA) and incubated at RT for a period between 5 and 15 minutes. Reaction was stopped by adding 100 µL of 0.5 M Sulfuric Acid. Reading is performed on Spectra Max 250 at 450 nm with reference at 750 nm. The method has been validated in mouse and rabbit plasma over a range of 20 - 200 ng/mL, in tumor mass over the range of 50 - 3200 ng/mL and in mouse liver over the range of 100 - 3200 ng/mL.

Pharmacokinetic analysis

Pharmacokinetics analysis was performed using a noncompartmental approach in Phoenix WinNonlin 6.3 (Pharsight Corporation, USA). All concentration data points were weighted by the inverse square of the fitted value. The following parameters were evaluated: time to reach maximum concentration (T_{max}), highest concentration (C_{max}), area under curve (AUC), elimination half-time ($t_{1/2\ elim}$), volume of distribution (V_d), total clearance (Cl_b), bioavailability (F%).

Peak concentration (C_{max}) and the time to reach C_{max} (T_{max}) after administration of the PNA were determined from the observed data. The area under curve (AUC) was calculated using the linear trapezoidal rule (calculation method linear trapezoidal with linear interpolation). The first order constant (λ_z) associated with the terminal (log-linear) portion of the curve was estimated by linear regression of time vs. log concentration and the terminal half-life was calculated as $\ln(2)/\lambda_z$. The volume of distribution (V_d) was calculated based on the terminal phase as Dose/ $\lambda_z \cdot$AUCINF_obs (where AUCINF_obs is the AUC from the time of dosing extrapolated to infinity). The total clearance (Cl_b) was calculated as Dose/AUCINF_obs. The bioavailability (F) after subcutaneous administration was calculated as the ratio of the AUC after subcutaneous (AUCsc) and intravenous (AUCiv) administration as (AUCsc/AUCiv) multiplied by 100.

Biodistribution of BGA002 in mice (QWBA-Charles River/Selcia)

The [^{14}C]-Ac-BGA002 (Batch No. 8249DCP006-6, radiochemical purity 99.8%) was supplied by Selcia Limited (UK) as a solution in acetic acid: sodium acetate: HCl (75 mM: 25 mM: 3.6 mM) with 2.5% mannitol at a concentration of 1.16 MBq/mL (3.35 mg [^{14}C]-Ac-BGA002 /mL). The solution was stored in a fridge set to maintain a temperature of +4°C. CD-1 mice (28-35 days of age) were supplied by Charles River, UK and acclimatized to the experimental unit for 7 days prior to use on the study. The [^{14}C]-Ac-BGA002 formulation was administered by injection into the nape of the neck (single subcutaneous administration) of 6 male and 6 female mice at a target volume of 4.5 mL/kg, to achieve a nominal dose level of 15 mg/kg (target radioactive dose of 5 MBq/kg). One male and one female mouse were humanely killed by CO_2 narcosis at each of 1, 4, 8, 24, 48 and 168 h post dose.

The carcass of each animal was then frozen by immersion in a mixture of solid CO_2 in hexane for ca 15 min. The frozen carcass was then embedded in a block of carboxymethylcellulose, which was frozen in the same way. After equilibration at -20°C, sagittal sections (30 µm thick) were taken through each animal using a whole body cryomicrotome (Leica Instruments GmbH). The sections were freeze dried prior to storage at ambient temperature. All samples prepared in scintillation fluid were subjected to liquid scintillation counting (LSC) for 5 min, together with representative blank samples, using a Liquid Scintillation Analyzer with automatic quench correction by an external method. Where possible, samples were analyzed in duplicate and allowed to heat and light stabilize prior to analysis. Prior to calculation of each result, a background count rate was determined and subtracted from each sample count rate. For scintillation counting, a limit of reliable measurement (LRM) of 30 c.p.m. above background has been instituted in these laboratories. Where results have arisen from data below the LRM, the fact is noted. The radioactivity present in various organs and tissues in whole body sections was determined by QWBA using a Typhoon FLA7000 scanner and AIDA image analysis software (version 4.06, raytest isotopenmeβgerate GmbH, Germany). For

analysis, representative whole-body sections were placed into close contact with phosphor screens and left for a period of 7 days. On each phosphor screen, a set of external standards was also exposed. These standards were prepared from blood spiked with a serial dilution of a [^{14}C]-labeled reference solution, which was dispensed into holes drilled into a block of carboxymethylcellulose, frozen and then sectioned in the same way as the animal samples. After the phosphor screen was scanned, an image of the radioactivity in the sample was stored digitally. For quantitative analysis, six background areas were defined on each storage phosphor screen image. The software automatically calculated the mean background and subsequently subtracted this from all standards and tissues analyzed. A regression coefficient was derived by comparing the response of each standard with the nominal concentration over the range of radioactive concentrations used and forcing the response curve through the origin. The concentrations of the standards used were in the range of 0.05 to 258.48 µg equiv/g. The response curve is linear over these concentrations and was assumed to be linear to the limit of reliable determination. Each organ or tissue of interest was then identified and integrated, and the software automatically calculated the concentration (µg equiv/g) using the regression equation derived from the standards.

The limit of reliable measurement for each storage screen was calculated from the assessment of the mean background of the plate and defined as 3 times the standard deviation of the mean above background. At the specific activity used in this study, the limit of reliable measurement was in the range of 0.01 to 0.04 µg equiv/g.

Xenograft mouse models

Neuroblastoma luminescent cells (Kelly-luc) and xenograft ectopic neuroblastoma mouse models were prepared according to previously published studies[2]. Small Cell Lung Cancer and Rhabdomyosarcoma xenograft ectotopic mouse models were prepared with the same method starting from H69AR-Luc and RMZ-Luc cell lines respectively. Kelly cell line was originally established from a 1 year old female patient with a stage IV NB with MYCN amplification and it has been purchased

from DSMZ (DSMZ Cat# ACC-355, RRID:CVCL_2092). The Alveolar Rhabdomyosarcoma cell line RMZ was kindly provided by Prof. Lollini (Department of Experimental Pathology at University of Bologna), and is characterized by MYCN amplification[35]. The Small Cell Lung Cancer H69AR cell line has been originally established from the pleural fluid of a 55 year old Caucasian male with small cell carcinoma of the lung and it has been purchased from ATCC (CRL-11351). The H69AR cell line is a multiple drug resistant cell line as compared to the parental NCI-H69 cell line. The H69AR cell line presents MYCN gene amplification, and high expression of MYCN mRNA and protein[36,37].

Pharmacokinetics evaluation of BGA002 in tumor and liver of xenograft NB, RMS and SCLC mouse models

NB, SCLC and RMS mouse models were established as described above. In each mouse model, systemic treatment with BGA002 was administered subcutaneously and started when specific bioluminescent value (in NB and SCLC mouse model), or tumor volume (in RMS mouse model) was reached. When the starting point was reached, NB mouse model was treated with BGA002 daily at 10 mg/kg/day or vehicle for 15 consecutively days, SCLC was treated with BGA002 at 15 mg/kg/day or vehicle for 9 consecutive days, while RMS was treated with BGA002 at 15 mg/kg/day or vehicle for 7, 8, 15, 20, 27, 34, 44, 49 days. Tumors and livers were extracted immediately after animal euthanasia, weighted on a precision scale and homogenized with a probe sonicator in RIPA extraction buffer at concentration of 10 mg/mL. Concentrations of BGA002 in tumor and liver were evaluated by the hybridization-based ELISA assay as described above. Samples were stored frozen at -20°C.

Pharmacodynamics evaluation of BGA002 in RMS and SCLC mouse models

SCLC and RMS mouse models were established as described above. In both cases, treatment was administered subcutaneously and started when specific tumor volume (in RMS mouse model), or

bioluminescent value (in SCLC mouse model) was reached. RMS mouse model was treated with BGA002 at the dose of 15 mg/kg/day for (n=4) or vehicle (n=5) for 14 consecutive days, while SCLC mouse model was treated with BGA002 at 5 mg/kg/day (n=4), 15 mg/kg/day (n=3), or vehicle (n=14) for 14 consecutive days. Twenty-four hours after the last injection, animals were euthanized and necropsy was performed.

Tumors were extracted and weighted on a precision scale and all organs collected for subsequent analysis and studies. Western blot Production of N-Myc protein was assessed in total protein extracts. Sample was removed from animal as quickly as possible after animal sacrifice and homogenized with a probe sonicator on ice in sample lysing solution added with a Halt protease inhibitor cocktail (Cat# 78429, Thermofisher) in a 1:100 rate. Sample lysing solution volume must be at least 200 uL and at maximum 2 mL and adjusted to a concentration of 100 mg/mL; Total protein extract was quantified with BCA method at NanoDrop ND-1000 spectrophotometer against a standard curve of BSA in sample lysing solution. Proteins were separated by one-dimensional precast polyacrylamide gel [Bolt Bis-Tris Plus Gels 10%], that provides a neutral pH environment with the aim to minimize protein modifications, under denaturing conditions. Samples containing 10 to 50 µg of proteins were denatured by incubation at 95°C for 10 min after the addition of 4X Sample buffer, 10X Reducing Agent and water to a final volume of 30 µL. Samples were loaded and run at 200 V for about 15 min in electrophoresis buffer [Bolt MES SDS Running buffer] with the molecular weight marker SeeBlue Plus2 Pre-Stained Standard. They were transferred from gel to PVDF membrane [IBlot Transfer Stack] using the IBlot Gel Transfer Device, a dry system that transfers proteins in 7 minutes [all materials and reagent were purchased from Life Technologies]. The membrane was subjected to overnight incubation at 4°C with blocking solution (5% milk in PBS-Tween 0.1%). The day after it was incubated 1 hour with primary antibody, a mouse monoclonal anti-N-Myc antibody [SC-53993_Santa Cruz] diluted 1:200 in 3.5% BSA in PBS-Tween 0.1%. After three washes in PBS-Tween 0.1%, the membrane was incubated one hour with the corresponding secondary antibody, a sheep anti-mouse IgG-HRP [Amersham Biosciences] diluted 1:10,000 in 3.5%

BSA in PBS-Tween 0.1%. The membrane was washed 3 times in PBS-Tween 0.1% for 5 min before detection. N-Myc chemiluminescent signal was measured adding the ECL Select Western Blotting solution [GE Healthcare] at ChemiDoc-It [UVP] to the membrane. The signal quantification was carried out with Alliance software [Uvitec] and was performed following colloidal staining with Coomassie brilliant blue dyes. Immunohistochemistry analysis Immunohistochemistry was performed on formaldehyde fixed and paraffin embedded samples, cut on microtome. Antigen retrieval was performed with EDTA-NaOH. Antibody used were Anti-MYCN primary antibody (OP13 Calbiochem) and HRP conjugated secondary antibody (Dako). Staining was performed with the DAKO kit for HRP Colorimetric revelation using DAB and Haematoxylin contrast.

Statistical analyses

All statistical analysis were performed using GraphPad Prism software (GraphPad Software Inc.) version 6. Data from distinct groups were compared using the MannWhitney test. $P < 0.05$ was considered significant.

DATA AND AVAILABILITY STATEMENT

ACKNOWLEDGEMENTS

We would like to thank Wissem Eljeder for suggestion and comments. We would like to thank the following CRO for their skilled support: Glp Life Test, Charles River, Selcia, Aptuit, Farefarma and WilResearch (now Charles River).

AUTHOR CONTRIBUTIONS

A.S. carried out data curation, project administration and participated in the writing, in study conceptualization and design. D.B. participated in study supervision, in the writing, validation, in formal analysis and in investigation. L.M. participated in developing the methodology, data acquisi-

tion, validation and reviewed the manuscript. S.B. participated in the investigation, in validation, in visualization and in the writing. S.A. and C.A. participated in administrative, technical and material support. G.N. and L.C. developed the chemical synthesis of the compound. S.O. and O.DP. revised the manuscript and participated in administrative, technical, and material support. A.P. and P.H. participated in funding acquisition, manuscript revision and study supervision. R.T. participated in study design and conceptualization, funding acquisition, manuscript revision and study supervision.

DECLARATION OF INTERESTS

R. Tonelli and A. Pession are BIOGENERA shareholders. A.L. Scardovi, worked for BIOGENERA at the time of the studies, she is currently working for Ritrova Therapeutics, Inc. D. Bartolucci, S. Bortolotti, S. Angelucci, C. Amadesi, G. Nieddu, and L. Cerisoli are working at BIOGENERA. No potential conflicts of interest were disclosed by the other authors.

KEYWORDS

MYCN-positive tumors, antigene PNA-peptide, pharmacokinetics, biodistribution, pharmacodynamics

REFERENCES

1. Liu, Z., Chen, S.S., Clarke, S., Veschi, V., and Thiele, C.J. (2020). Targeting MYCN in Pediatric and Adult Cancers. Front Oncol *10*, 623679. 10.3389/fonc.2020.623679.

2. Montemurro, L., Raieli, S., Angelucci, S., Bartolucci, D., Amadesi, C., Lampis, S., Scardovi, A.L., Venturelli, L., Nieddu, G., Cerisoli, L., et al. (2019). A Novel MYCN-Specific Antigene Oligonucleotide Deregulates Mitochondria and Inhibits Tumor Growth in MYCN-Amplified Neuroblastoma. Cancer Res *79*, 6166–6177. 10.1158/0008-5472.CAN-19-0008.

3. Bartolucci, D., Montemurro, L., Raieli, S., Lampis, S., Pession, A., Hrelia, P., and Tonelli, R. (2022). MYCN Impact on High-Risk Neuroblastoma: From Diagnosis and Prognosis to Targeted Treatment. Cancers (Basel) *14*, 4421. 10.3390/cancers14184421.

4. Tonelli, R., McIntyre, A., Camerin, C., Walters, Z.S., Di Leo, K., Selfe, J., Purgato, S., Missiaglia, E., Tortori, A., Renshaw, J., et al. (2012). Antitumor activity of sustained N-myc re-

duction in rhabdomyosarcomas and transcriptional block by antigene therapy. Clin Cancer Res *18*, 796–807. 10.1158/1078-0432.CCR-11-1981.

5. Peifer, M., Fernández-Cuesta, L., Sos, M.L., George, J., Seidel, D., Kasper, L.H., Plenker, D., Leenders, F., Sun, R., Zander, T., et al. (2012). Integrative genome analyses identify key somatic driver mutations of small-cell lung cancer. Nat Genet *44*, 1104–1110. 10.1038/ng.2396.

6. George, J., Lim, J.S., Jang, S.J., Cun, Y., Ozretić, L., Kong, G., Leenders, F., Lu, X., Fernández-Cuesta, L., Bosco, G., et al. (2015). Comprehensive genomic profiles of small cell lung cancer. Nature *524*, 47–53. 10.1038/nature14664.

7. Beltran, H., Rickman, D.S., Park, K., Chae, S.S., Sboner, A., MacDonald, T.Y., Wang, Y., Sheikh, K.L., Terry, S., Tagawa, S.T., et al. (2011). Molecular characterization of neuroendocrine prostate cancer and identification of new drug targets. Cancer Discov *1*, 487–495. 10.1158/2159-8290.CD-11-0130.

8. Zimmerman, K.A., Yancopoulos, G.D., Collum, R.G., Smith, R.K., Kohl, N.E., Denis, K.A., Nau, M.M., Witte, O.N., Toran-Allerand, D., and Gee, C.E. (1986). Differential expression of myc family genes during murine development. Nature *319*, 780–783. 10.1038/319780a0.

9. Fletcher, J.I., Ziegler, D.S., Trahair, T.N., Marshall, G.M., Haber, M., and Norris, M.D. (2018). Too many targets, not enough patients: rethinking neuroblastoma clinical trials. Nat Rev Cancer *18*, 389–400. 10.1038/s41568-018-0003-x.

10. Wolpaw, A.J., Bayliss, R., Büchel, G., Dang, C.V., Eilers, M., Gustafson, W.C., Hansen, G.H., Jura, N., Knapp, S., Lemmon, M.A., et al. (2021). Drugging the "Undruggable" MYCN Oncogenic Transcription Factor: Overcoming Previous Obstacles to Impact Childhood Cancers. Cancer Res *81*, 1627–1632. 10.1158/0008-5472.CAN-20-3108.

11. Tonelli, R., Purgato, S., Camerin, C., Fronza, R., Bologna, F., Alboresi, S., Franzoni, M., Corradini, R., Sforza, S., Faccini, A., et al. (2005). Anti-gene peptide nucleic acid specifically inhibits MYCN expression in human neuroblastoma cells leading to cell growth inhibition and apoptosis. Mol Cancer Ther *4*, 779–786. 10.1158/1535-7163.MCT-04-0213.

12. Astolfi, A., Vendemini, F., Urbini, M., Melchionda, F., Masetti, R., Franzoni, M., Libri, V., Serravalle, S., Togni, M., Paone, G., et al. (2014). MYCN is a novel oncogenic target in pediatric T-cell acute lymphoblastic leukemia. Oncotarget *5*, 120–130. 10.18632/oncotarget.1337.

13. Bortolotti, S., Angelucci, S., Montemurro, L., Bartolucci, D., Raieli, S., Lampis, S., Amadesi, C., Scardovi, A., Nieddu, G., Cerisoli, L., et al. (2023). Antigene MYCN Silencing by BGA002 Inhibits SCLC Progression Blocking mTOR Pathway and Overcomes Multidrug Resistance. Cancers (Basel) *15*, 990. 10.3390/cancers15030990.

14. Lampis, S., Raieli, S., Montemurro, L., Bartolucci, D., Amadesi, C., Bortolotti, S., Angelucci, S., Scardovi, A.L., Nieddu, G., Cerisoli, L., et al. (2022). The MYCN inhibitor BGA002 restores the retinoic acid response leading to differentiation or apoptosis by the mTOR block in MYCN-amplified neuroblastoma. J Exp Clin Cancer Res *41*, 160. 10.1186/s13046-022-02367-5.

15. Pession, A., Tonelli, R., Fronza, R., Sciamanna, E., Corradini, R., Sforza, S., Tedeschi, T., Marchelli, R., Montanaro, L., Camerin, C., et al. (2004). Targeted inhibition of NMYC by pep-

tide nucleic acid in N-myc amplified human neuroblastoma cells: cell-cycle inhibition with induction of neuronal cell differentiation and apoptosis. Int J Oncol *24*, 265–272.

16. Nielsen, P.E., Egholm, M., Berg, R.H., and Buchardt, O. (1991). Sequence-selective recognition of DNA by strand displacement with a thymine-substituted polyamide. Science *254*, 1497–1500. 10.1126/science.1962210.

17. Janowski, B.A., Huffman, K.E., Schwartz, J.C., Ram, R., Hardy, D., Shames, D.S., Minna, J.D., and Corey, D.R. (2005). Inhibiting gene expression at transcription start sites in chromosomal DNA with antigene RNAs. Nat Chem Biol *1*, 216–222. 10.1038/nchembio725.

18. Wancewicz, E.V., Maier, M.A., Siwkowski, A.M., Albertshofer, K., Winger, T.M., Berdeja, A., Gaus, H., Vickers, T.A., Bennett, C.F., Monia, B.P., et al. (2010). Peptide nucleic acids conjugated to short basic peptides show improved pharmacokinetics and antisense activity in adipose tissue. J Med Chem *53*, 3919–3926. 10.1021/jm901489k.

19. Volpi, S., Cancelli, U., Neri, M., and Corradini, R. (2020). Multifunctional Delivery Systems for Peptide Nucleic Acids. Pharmaceuticals (Basel) *14*, 14. 10.3390/ph14010014.

20. Cutrona, G., Carpaneto, E.M., Ulivi, M., Roncella, S., Landt, O., Ferrarini, M., and Boffa, L.C. (2000). Effects in live cells of a c-myc anti-gene PNA linked to a nuclear localization signal. Nat Biotechnol *18*, 300–303. 10.1038/73745.

21. Boffa, L.C., Cutrona, G., Cilli, M., Mariani, M.R., Matis, S., Pastorino, M., Damonte, G., Millo, E., Roncella, S., and Ferrarini, M. (2005). Therapeutically promising PNA complementary to a regulatory sequence for c-myc: pharmacokinetics in an animal model of human Burkitt's lymphoma. Oligonucleotides *15*, 85–93. 10.1089/oli.2005.15.85.

22. Sazani, P., Gemignani, F., Kang, S.-H., Maier, M.A., Manoharan, M., Persmark, M., Bortner, D., and Kole, R. (2002). Systemically delivered antisense oligomers upregulate gene expression in mouse tissues. Nat Biotechnol *20*, 1228–1233. 10.1038/nbt759.

23. Ganguly, S., Chaubey, B., Tripathi, S., Upadhyay, A., Neti, P.V.S.V., Howell, R.W., and Pandey, V.N. (2008). Pharmacokinetic analysis of polyamide nucleic-acid-cell penetrating peptide conjugates targeted against HIV-1 transactivation response element. Oligonucleotides *18*, 277–286. 10.1089/oli.2008.0140.

24. Mier, W., Eritja, R., Mohammed, A., Haberkorn, U., and Eisenhut, M. (2003). Peptide-PNA conjugates: targeted transport of antisense therapeutics into tumors. Angew Chem Int Ed Engl *42*, 1968–1971. 10.1002/anie.200219978.

25. Albertshofer, K., Siwkowski, A.M., Wancewicz, E.V., Esau, C.C., Watanabe, T., Nishihara, K.C., Kinberger, G.A., Malik, L., Eldrup, A.B., Manoharan, M., et al. (2005). Structure-activity relationship study on a simple cationic peptide motif for cellular delivery of antisense peptide nucleic acid. J Med Chem *48*, 6741–6749. 10.1021/jm050490b.

26. McMahon, B.M., Mays, D., Lipsky, J., Stewart, J.A., Fauq, A., and Richelson, E. (2002). Pharmacokinetics and tissue distribution of a peptide nucleic acid after intravenous administration. Antisense Nucleic Acid Drug Dev *12*, 65–70. 10.1089/108729002760070803.

27. Bennett, C.F., and Swayze, E.E. (2010). RNA targeting therapeutics: molecular mechanisms of antisense oligonucleotides as a therapeutic platform. Annu Rev Pharmacol Toxicol *50*, 259–293. 10.1146/annurev.pharmtox.010909.105654.

28. Faccini, A., Tortori, A., Tedeschi, T., Sforza, S., Tonelli, R., Pession, A., Corradini, R., and Marchelli, R. (2008). Circular dichroism study of DNA binding by a potential anticancer peptide nucleic acid targeted against the MYCN oncogene. Chirality *20*, 494–500. 10.1002/chir.20489.

29. Hatzi, E., Breit, S., Zoephel, A., Ashman, K., Tontsch, U., Ahorn, H., Murphy, C., Schweigerer, L., and Fotsis, T. (2000). MYCN oncogene and angiogenesis: down-regulation of endothelial growth inhibitors in human neuroblastoma cells. Purification, structural, and functional characterization. Adv Exp Med Biol *476*, 239–248. 10.1007/978-1-4615-4221-6_19.

30. Ribatti, D., Raffaghello, L., Pastorino, F., Nico, B., Brignole, C., Vacca, A., and Ponzoni, M. (2002). In vivo angiogenic activity of neuroblastoma correlates with MYCN oncogene overexpression. International Journal of Cancer *102*, 351–354. 10.1002/ijc.10742.

31. DeLONG, R. k., Nolting, A., Fisher, M., Chen, Q., Wickstrom, E., Kligshteyn, M., Demirdji, S., Caruthers, M., and Juliano, R. l. (1997). Comparative Pharmacokinetics, Tissue Distribution, and Tumor Accumulation of Phosphorothioate, Phosphorodithioate, and Methylphosphonate Oligonucleotides in Nude Mice. Antisense and Nucleic Acid Drug Development *7*, 71–77. 10.1089/oli.1.1997.7.71.

32. Wang, H., Rayburn, E.R., Wang, W., Kandimalla, E.R., Agrawal, S., and Zhang, R. (2006). Immunomodulatory oligonucleotides as novel therapy for breast cancer: pharmacokinetics, in vitro and in vivo anticancer activity, and potentiation of antibody therapy. Molecular Cancer Therapeutics *5*, 2106–2114. 10.1158/1535-7163.MCT-06-0158.

33. Devi, G.R., Beer, T.M., Corless, C.L., Arora, V., Weller, D.L., and Iversen, P.L. (2005). In vivo Bioavailability and Pharmacokinetics of a c-MYC Antisense Phosphorodiamidate Morpholino Oligomer, AVI-4126, in Solid Tumors. Clinical Cancer Research *11*, 3930–3938. 10.1158/1078-0432.CCR-04-2091.

34. Bartolucci, D., Pession, A., Hrelia, P., and Tonelli, R. (2022). Precision Anti-Cancer Medicines by Oligonucleotide Therapeutics in Clinical Research Targeting Undruggable Proteins and Non-Coding RNAs. Pharmaceutics *14*, 1453. 10.3390/pharmaceutics14071453.

35. Toffolatti, L., Frascella, E., Ninfo, V., Gambini, C., Forni, M., Carli, M., and Rosolen, A. (2002). MYCN expression in human rhabdomyosarcoma cell lines and tumour samples. J Pathol *196*, 450–458. 10.1002/path.1068.

36. Johnson, B.E., Ihde, D.C., Makuch, R.W., Gazdar, A.F., Carney, D.N., Oie, H., Russell, E., Nau, M.M., and Minna, J.D. (1987). myc family oncogene amplification in tumor cell lines established from small cell lung cancer patients and its relationship to clinical status and course. J Clin Invest *79*, 1629–1634. 10.1172/JCI112999.

37. Kiefer, P.E., Bepler, G., Kubasch, M., and Havemann, K. (1987). Amplification and Expression of Protooncogenes in Human Small Cell Lung Cancer Cell Lines. Cancer Research *47*, 6236–6242.

LIST OF FIGURE CAPTIONS/LEGENDS

Figure 1. BGA002 pharmacokinetics in plasma of mice and rabbits. (A) Plasma concentration–time profiles of BGA002 over 8 hours in male and female murine blood, after a single intravenous injection with BGA002 at 15 mg/kg. (B) Plasma concentration–time profiles of BGA002 over 8 hours in male and female murine blood, after a single subcutaneous injection with BGA002 at 15 mg/kg. (C) Comparison of plasma concentration–time profiles between IV and SC administration routes in murine blood, after single treatment with BGA002 at 15 mg/kg. (D) Comparison of plasma concentration–time profiles in murine blood obtained after one day and after 28 days of once-daily repeated SC administration of BGA002 at 2.5 mg/kg. (E) Plasma concentration–time profiles in murine blood over 8 hours after single SC administration with BGA002 at 2.5 mg/kg, 7.5 mg/kg and 25 mg/kg. In all the studies, due to technical sample limitation in juvenile animals, for each timepoint the samples from three different animals were pooled in a single tube and analyzed through hybridization-based ELISA.

Figure 2. BGA002 biodistribution in male and female mice after single SC administration. (A) Biodistribution in wild type mice up to seven days after SC administration of [^{14}C]-Ac-BGA002 (15 mg/kg). Organs and tissues are divided in three groups. BGA002 concentration is reported as percentage of ug equiv/g normalized within each group. (B) Biodistribution of [^{14}C]-Ac-BGA002 is reported as mean from male and female values for specific organ of interest. As expected, higher values can be found in kidney and liver, where oligonucleotides are commonly accumulated. (C) Example of radiographic section image of biodistribution in mouse (female) after eight hours after single SC administration of [^{14}C]-Ac-BGA002 (15 mg/kg).

Figure 3. BGA002 localizes in different MNA-positive tumors. PK concentration in tumor and liver in MNA-positive SCLC, NB and RMS mouse models, after systemic SC administration with BGA002 at 15 mg/kg for 9 days (in SCLC), 10 mg/kg for 15 days (in NB) and 15 mg/kg for 15 days (in RMS). Mean value for SCLC are respectively N= 120 μg/g and N=273 μg/g (*p*-value =

0.0072); Mean values for NB are respectively N= 360.6 μg/g and N=111.9 μg/g (*p*-value = 0.0424); Mean values for RMS are respectively N= 121.4 μg/g and N=754.6 μg/g (*p*-value = 0.1000). Mann-Whitney test was performed for statistical analysis (ns = *p*-value > 0.05; * = *p*-value ≤ 0.05; ** = *p*-value ≤ 0.01).

Figure 4. BGA002 induces reduction in tumor weight and N-Myc protein in MNA-positive tumor mouse models. (A) Evaluation by bioluminescence and immunohistochemistry (reconstruction and magnification) of tumor growth after 15 days of once daily systemic administration of BGA002 at 5 or 15 mg/kg/days in MNA-positive SCLC mouse model. Data are reported at the experiment end. (B). Tumor weight is reported at the end of experiment in SCLC and RMS, after 15 days of once daily SC administration of BGA002. Mean value for SCLC are respectively N= 313.1 mg, N=267.0 mg (*p*-value = 0.8944) and N= 128.7 (*p*-value = 0.0324); Mean values for RMS are respectively N= 303.6 mg and N=90.8 mg (*p*-value = 0.0635). (C) N-Myc protein levels are reported at the end of experiment in SCLC (*p*-value = 0.1905 and 0.1429) and RMS (*p*-value = 0.0178), after treatment with BGA002. Mann-Whitney test was performed for statistical analysis (ns = *p*-value > 0.05; * = *p*-value ≤ 0.05).

TABLES

Table 1 Pharmacokinetics parameters in mouse and rabbit.

Table reporting complete PK parameters calculated in mice .In order are reported data after subcutaneous (SC) or intravenous (IV) single dose administration in mouse and single versus repeated subcutaneous (SC) administration in mouse. Each value is reported as mean of multiple single values. Abbreviation: time to reach maximum concentration (T_{max}), highest concentration (C_{max}), area under curve (AUC_{0-t}), AUC from the time of dosing extrapolated to infinity (AUC_{inf}), elimination half-time ($t_{1/2\ elim}$), volume of distribution (V_d), total body clearance (Cl_b), bioavailability (F).

			Mouse single administration					Mouse repeated administration (SC)		
BGA002 Dose (mg/kg):			5.0		15.0			2.5	7.5	25
Parameter	Unit	Administration route	M	F	M	F	Day(s)	F	F	F
T_{max}	h	SC	0.16	0.50	0.50	0.16	1 Day	0.50	0.50	0.50
C_{max}	ng/ml		259	296	487	558		198	410	1031
$AUC_{(0-t)}$	h*ng/ml		566.07	408.80	1527.29	1545.21		478.17	1331.15	3433.62
AUC_{inf}	h*ng/ml		711.09	586.01	1775.22	1848.95		766.46	1601.45	3951.81
$t_{1/2\ elim}$	h		4.10	1.88	3.06	3.33		7.48	3.28	2.76
V_d	ml/kg		41621.48	23155.77	37342.78	38928.76		35218.41	22169.39	25217.22
Cl_b	mg/h/kg		7031.42	8532.22	8449.65	8112.69		3261.74	4683.26	6326.21
F	%		85.81	59.29	111.01	108.05				
T_{max}	h	IV	0.25	0.08	0.50	0.08	28 Days	0.50	0.17	0.17
C_{max}	ng/ml		520	571	492	557		182	356	1284
$AUC_{(0-t)}$	h*ng/ml		659.69	689.55	1375.77	1430.13		428.83	1208.7	2801.54
AUC_{inf}	h*ng/ml		742.48	761.47	1643.21	1601.74		652.03	1512.09	3378.25
$t_{1/2\ elim}$	h		1.43	1.31	3.75	2.80		6.19	3.42	3.20
V_d	ml/kg		13939.52	12363.09	49321.23	37815.86		34231.43	24468.71	34142.64
Cl_b	mg/h/kg		6734.15	6566.21	9128.45	9364.78		3834.19	4960.02	7400.28

Click here to access/download;Supplemental Information (PDF format);Supplementary Material.pdf

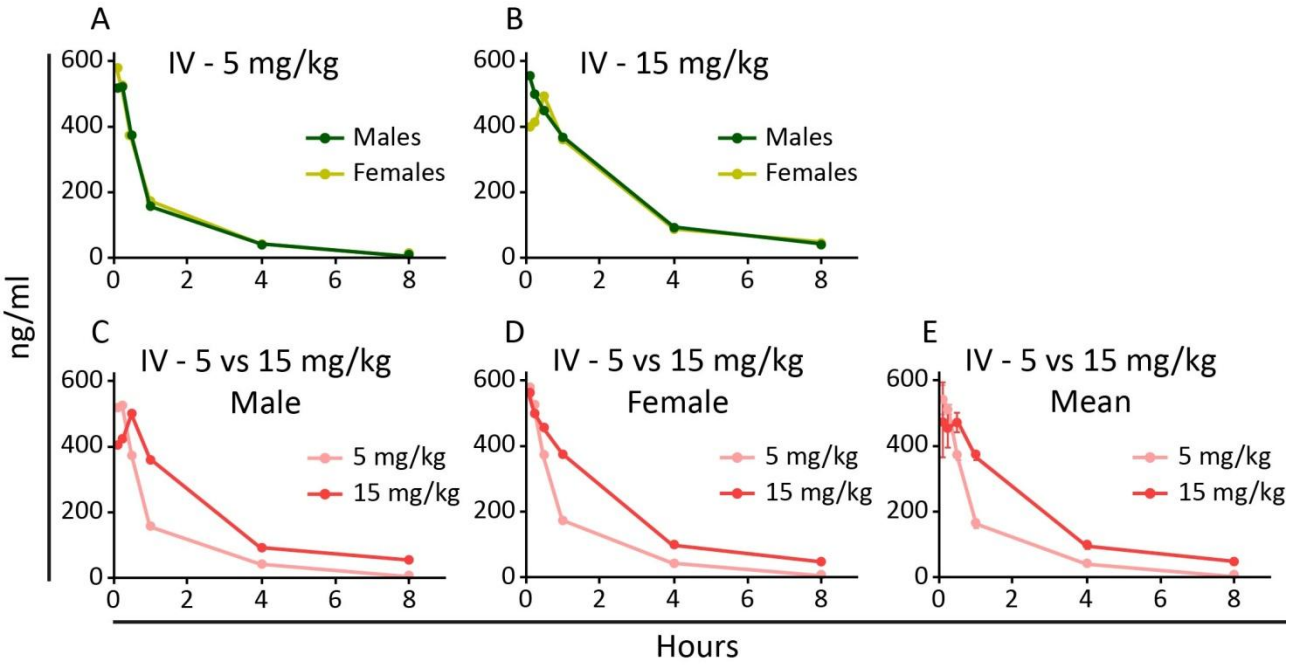

Figure S1. BGA002 pharmacokinetics in mice after single intravenous (IV) administration. Comparison of plasma concentration–time profiles of BGA002 over 8 hours in male and female murine blood, after single IV administration of BGA002 at 5 mg/kg (A) and 15 mg/kg (B). Comparison of plasma concentration–time profiles of BGA002 over 8 hours, after single IV administration of BGA002 at 5 mg/kg and 15 mg/kg in murine blood for males (C), females (D) and the mean of males and females (E). Data for male and female mice at each dose and time point are obtained by the analysis of plasma derived from the blood withdrawn from 3 animals and pooled in the same tube, thus standard deviation values are not available except for the figure E, where the average is calculated on the values of males and females.

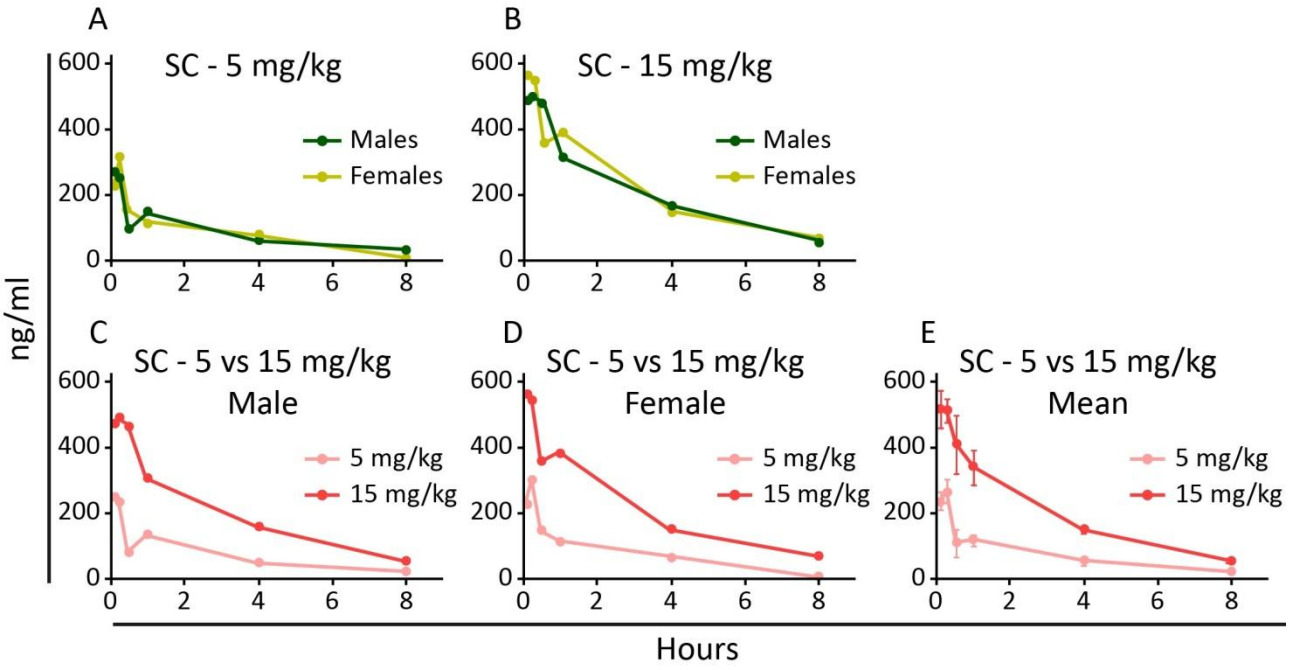

Figure S2. BGA002 pharmacokinetics in mice after single subcutaneous (SC) administration. Comparison of plasma concentration–time profiles of BGA002 over 8 hours in male and female murine blood, after single SC administration of BGA002 at 5 mg/kg (A) and 15 mg/kg (B). Comparison of plasma concentration-time profiles of BGA002 over 8 hours, after single SC administration of BGA002 at 5 mg/kg and 15 mg/kg in murine blood for males (C), females (D) and the mean of values from males and females (E). Data for male and female mice at each dose and time point are obtained by the analysis of plasma derived from the blood withdrawn from 3 animals and pooled in the same tube, thus standard deviation values are not available except for the figure E, where the average is calculated on the values of males and females.

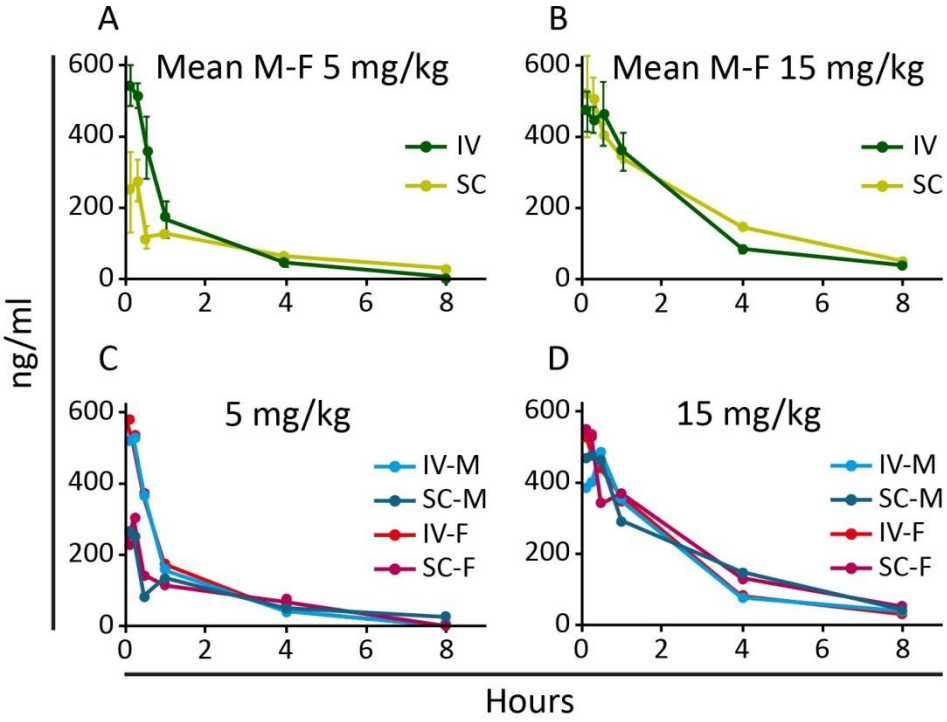

Figure S3. Comparison of BGA002 pharmacokinetics in mice after single subcutaneous (SC) and intravenous (IV) administration, in male and female mice. Comparison of plasma concentration–time profiles of BGA002 over 8 hours after single SC and IV administration of BGA002 at 5 mg/kg (A) 15 mg/kg (B) in male and female murine blood. Comparison of plasma concentration–time profiles of BGA002 over 8 hours after single SC and IV administration of BGA002 at 5 mg/kg (C) and 15 mg/kg (D) reported as mean values of males and females. Data for male and female mice at each dose and time point are obtained by the analysis of plasma derived from the blood withdrawn from 3 animals and pooled in the same tube, thus standard deviation values are not available except for the figure C and D, where the average is calculated on the values of males and females.

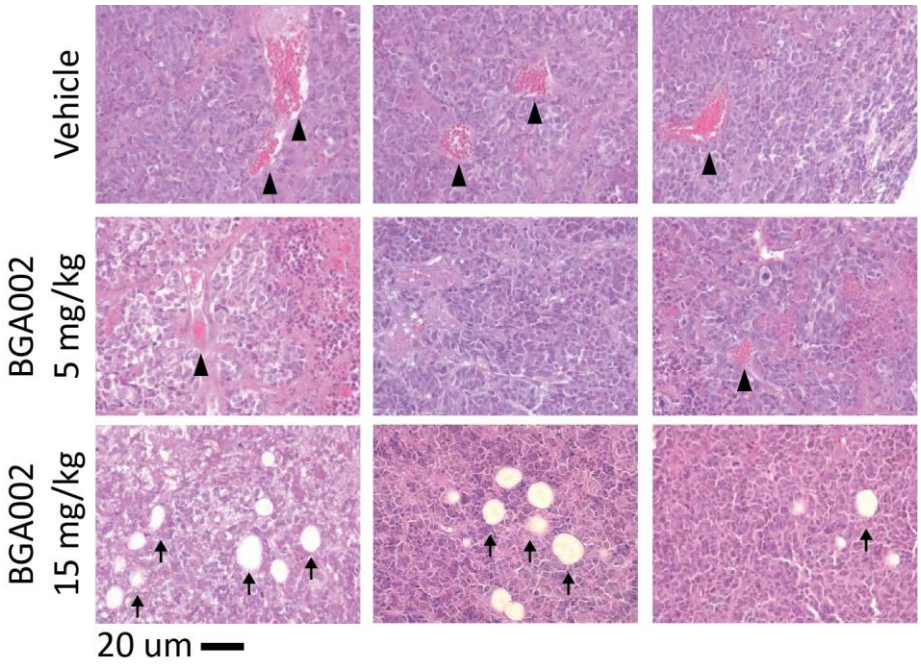

Figure S4. BGA002 inhibits vascularization and cellular density in SCLC tumor masses. Images of tumor masses sections shown are stained with hematoxylin and eosin, after 9 days of once daily systemic administration of BGA002 at 5 or 15 mg/kg/day in a multidrug resistant MNA-SCLC mouse model. Data are reported at the experiment end. Similar results were obtained from three independent mice. Black triangles indicate vascular structures, black arrows indicate areas of low cellular density.

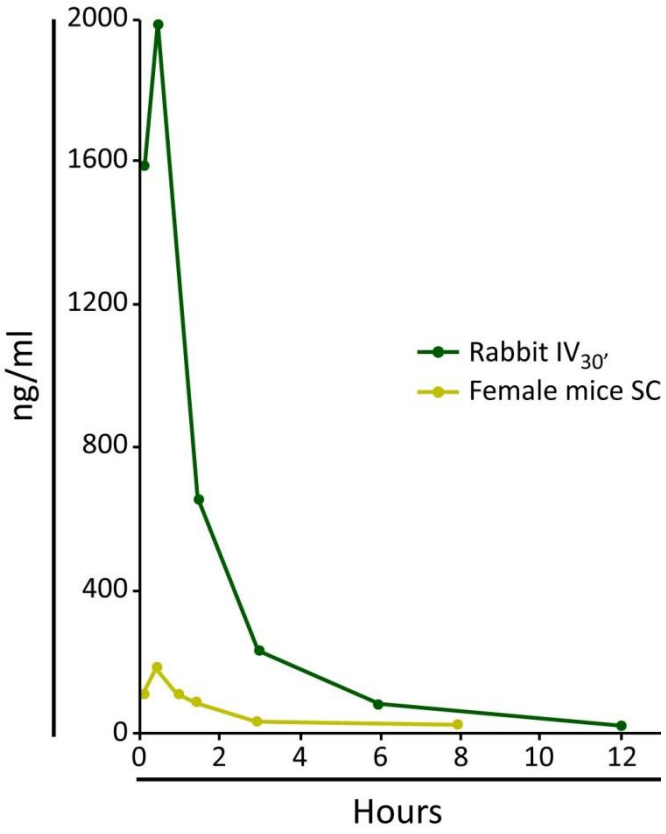

Figure S5. Comparison of plasma concentration in rabbit vs mouse. Comparison of plasma concentration–time profiles of BGA002 at 2.5 mg/kg, after single IV administration in rabbits versus SC administration in mice. For each timepoint the samples from three different animals were pooled in a single tube and analyzed through hybridization-based ELISA, due to technical sample limitation in juvenile animals.

Sex	Dose (mg/kg)	Timepoint (minutes)	Timepoint (hours)	BGA002 concentration in blood (ng/ml)
male	5	5	0,083	509
male	5	15	0,25	520
male	5	30	0,5	370
male	5	60	1	153
male	5	240	4	40
male	5	480	8	<LLOQ
female	5	5	0,083	571
female	5	15	0,25	501
female	5	30	0,5	357
female	5	60	1	170
female	5	240	4	38,2
female	5	480	8	<LLOQ
male	15	5	0,083	397
male	15	15	0,25	411
male	15	30	0,5	492
male	15	60	1	359
male	15	240	4	89,2
male	15	480	8	49,5
female	15	5	0,083	557
female	15	15	0,25	495
female	15	30	0,5	448
female	15	60	1	370
female	15	240	4	95
female	15	480	8	42,5

Table S1 BGA002 concentration in blood after single IV injection in mouse. Raw data of BGA002 blood concentration in mouse is reported for each time point in each sex and all doses tested. Data refers to single IV injection. Lower limit of quantitation (LLOQ).

Sex	Dose (mg/kg)	Timepoint (minutes)	Timepoint (hours)	BGA002 concentration in blood (ng/ml)
male	5	5	0,083	259
male	5	15	0,25	246
male	5	30	0,5	83,1
male	5	60	1	134
male	5	240	4	49,6
male	5	480	8	24,5
female	5	5	0,083	220
female	5	15	0,25	296
female	5	30	0,5	141
female	5	60	1	110
female	5	240	4	65,3
female	5	480	8	<LLOQ
male	15	5	0,083	478
male	15	15	0,25	487
male	15	30	0,5	474
male	15	60	1	306
male	15	240	4	160
male	15	480	8	56,1
female	15	5	0,083	558
female	15	15	0,25	538
female	15	30	0,5	349
female	15	60	1	379
female	15	240	4	144
female	15	480	8	63,3

Table S2 BGA002 concentration in blood after single SC injection in mouse. Raw data of BGA002 blood concentration in mouse is reported for each time point in each sex and all doses tested. Data refers to single SC injection. Lower limit of quantitation (LLOQ).

Dose (mg/kg)	Number of injection	Timepoint (minutes)	Timepoint (hours)	BGA002 concentration in blood (ng/ml)
25	1	10	0,17	731
25	1	30	0,5	1031
25	1	60	1	709
25	1	90	1,5	668
25	1	180	3	454
25	1	480	8	130
7,5	1	10	0,17	332
7,5	1	30	0,5	410
7,5	1	60	1	369
7,5	1	90	1,5	299
7,5	1	180	3	139
7,5	1	480	8	57,1
2,5	1	10	0,17	157
2,5	1	30	0,5	198
2,5	1	60	1	139
2,5	1	90	1,5	110
2,5	1	180	3	34
2,5	1	480	8	26,7
25	28	10	0,17	1284
25	28	30	0,5	576
25	28	60	1	433
25	28	90	1,5	588
25	28	180	3	346
25	28	480	8	125
7,5	28	10	0,17	356
7,5	28	30	0,5	280
7,5	28	60	1	134
7,5	28	90	1,5	227
7,5	28	180	3	171
7,5	28	480	8	61,5
2,5	28	10	0,17	113

2,5	28	30	0,5	182
2,5	28	60	1	117
2,5	28	90	1,5	91,6
2,5	28	180	3	34,6
2,5	28	480	8	25

Table S3 BGA002 concentration in blood after dose escalation in single or repeated SC injections in mouse. Raw data of BGA002 blood concentration in mouse is reported for each time point after single or 28 daily consecutive injections. BGA002 incremental doses range from 2.5 mg/kg to 25 mg/kg.

Dose (mg/kg)	Timepoint (minutes)	Timepoint (hours)	BGA002 concentration in blood (ng/ml)
2,5	10	0,17	1598
2,5	30	0,5	1989
2,5	90	1,5	656
2,5	180	3	231
2,5	360	6	82,2
2,5	720	12	22,6

Table S4 BGA002 concentration in blood after a 30 minutes IV infusion in rabbit. Raw data of BGA002 blood concentration in rabbit is reported for each time point after a 30 minutes IV infusion.

Parameter	Unit	Values
T_{max}	h	0.50
C_{max}	ng/ml	1989
$AUC_{(0-t)}$	h*ng/ml	3499.64
AUC_{inf}	h*ng/ml	3600.09
$t_{1/2\ elim}$	h	3.08
V_d	ml/kg	3086.70
Cl_b	mg/h/kg	694.43

Table S5 Summary of PK parameters after single IV administration in rabbit. Complete PK data are reported after single IV administration of BGA002 in male rabbit treated with BGA002 at 2.5 mg/kg. Each value is reported as mean of multiple single values. Abbreviations: time to reach maximum concentration (T_{max}), highest concentration (C_{max}), area under curve (AUC_{0-t}), AUC from the time of dosing extrapolated to infinity (AUC_{inf}), elimination half-time ($t_{1/2\ elim}$), volume of distribution (Vd), total body clearance (Clb).

SUPPLEMENTARY MATERIALS AND METHODS

Animals: rabbits

Pharmacokinetics plasma analysis was performed in juvenile rabbits (New Zealand White rabbit, LAGO: INRA 1077 (Nzw) EOPS) and Wil Research. Aptuit and Farefarma performed respectively ELISA analysis and pharmacokinetics analysis. Animals were maintained according to each CRO internal standard operating procedures.

In-vivo PK/TK experiments in rabbit plasma

The studies were conducted with the support of the following CRO:

- In-vivo phase : WIL Research Europe - Lyon SAS, 329 Impasse du Domaine Rozier, 69210 Saint-Germain-Nuelles, France (now Charles River)
- Bioanalysis: Aptuit Verona Srl, Via Alessandro Fleming, 4 - 37135 Verona, Italy
- Pharmacokinetic Analysis: Farefarma Srl, Via Ferrari, 9 - 28045 Invorio, Italy

The animals used for the studies include Male New Zealand White rabbit (LAGO: INRA 1077 (Nzw) EOPS) (6 weeks old at start of treatment) from Centre LAGO, 01540 Vonnas, France.

The rationale for the dose selection is based on mice studies as described in materials and methods. In particular, for rabbits, which are known to have generally a slower metabolism and a higher exposition when compared to mice, the chosen dose was 2.5 mg/kg. Rabbits were treated with a 30-minute intravenous infusion of 2.5 mg/kg BGA002 (volume administered: 0.625 mL/kg/day and rate of dosing: 1.25 mL/kg/h) using a microflex infusion set introduced into an ear vein (a preliminary compatibility test demonstrated that no compound was retained by the infusion system). Sampling time-points (6 time-points): 10, 30 (before the end of infusion) and 90 minutes, and 3, 6 and 12 hours. Blood sampling time-points were considered from the start of infusion. Blood was sampled individually from the 3 rabbits and plasma was pooled for all 3 animals per time-point.

Control pooled mouse and rabbit plasma (Lithium Heparin-LiHe) are centrifuged for approximately 10 minutes at 3000xg prior to use.

Figures

Click here to access/download

ZIP File

Figures.7z

CellPress

CELL PRESS DECLARATION OF INTERESTS POLICY

Transparency is essential for a reader's trust in the scientific process and for the credibility of published articles. At Cell Press, we feel that disclosure of competing interests is a critical aspect of transparency. Therefore, we require a "declaration of interests" section in which all authors disclose any financial or other interests related to the submitted work that (1) could affect or have the perception of affecting the author's objectivity or (2) could influence or have the perception of influencing the content of the article.

What types of articles does this apply to?

We require that you disclose competing interests for all submitted content by completing and submitting the form below. We also require that you include a "declaration of interests" section in the text of all articles even if there are no interests to declare.

What should I disclose?

We require that you and all authors disclose any personal financial interests (e.g., stocks or shares in companies with interests related to the submitted work or consulting fees from companies that could have interests related to the work), professional affiliations, advisory positions, board memberships (including membership on a journal's advisory board when publishing in that journal), or patent holdings that are related to the subject matter of the contribution. As a guideline, you need to declare an interest for (1) any affiliation associated with a payment or financial benefit exceeding $10,000 p.a. or 5% ownership of a company or (2) research funding by a company with related interests. You do not need to disclose diversified mutual funds, 401ks, or investment trusts.

Authors should also disclose relevant financial interests of immediate family members. Cell Press uses the Public Health Service definition of "immediate family member," which includes spouse and dependent children.

Where do I declare competing interests?

Competing interests should be disclosed on this form as well as in a "declaration of interests" section in the manuscript. This section should include financial or other competing interests as well as affiliations that are not included in the author list. Examples of "declaration of interests" language include:

> "AUTHOR is an employee and shareholder of COMPANY."
> "AUTHOR is a founder of COMPANY and a member of its scientific advisory board."

NOTE: Primary affiliations should be included with the author list and do not need to be included in the "declaration of interests" section. Funding sources should be included in the "acknowledgments" section and also do not need to be included in the "declaration of interests" section. (A small number of front-matter article types do not include an "acknowledgments" section. For these articles, reporting of funding sources is not required.)

What if there are no competing interests to declare?

If you have no competing interests to declare, please note that in the "declaration of interests" section with the following wording:

> "The authors declare no competing interests."

CELL PRESS DECLARATION OF INTERESTS FORM

If submitting materials via Editorial Manager, please complete this form and upload with your initial submission. Otherwise, please email as an attachment to the editor handling your manuscript.

Please complete each section of the form and insert any necessary "declaration of interests" statement in the text box at the end of the form. A matching statement should be included in a "declaration of interests" section in the manuscript.

Institutional affiliations

We require that you list the current institutional affiliations of all authors, including academic, corporate, and industrial, on the title page of the manuscript. ***Please select one of the following:***

☒ All affiliations are listed on the title page of the manuscript.

☐ I or other authors have additional affiliations that we have noted in the "declaration of interests" section of the manuscript and on this form below.

Funding sources

We require that you disclose all funding sources for the research described in this work. ***Please confirm the following:***

☒ All funding sources for this study are listed in the "acknowledgments" section of the manuscript.*

*A small number of front-matter article types do not include an "acknowledgments" section. For these, reporting funding sources is not required.

Competing financial interests

We require that authors disclose any financial interests and any such interests of immediate family members, including financial holdings, professional affiliations, advisory positions, board memberships, receipt of consulting fees, etc., that:

(1) could affect or have the perception of affecting the author's objectivity, *or*
(2) could influence or have the perception of influencing the content of the article.

Please select one of the following:

☒ We, the authors and our immediate family members, have no financial interests to declare.

☐ We, the authors, have noted any financial interests in the "declaration of interests" section of the manuscript and on this form below, and we have noted interests of our immediate family members.

Advisory/management and consulting positions

We require that authors disclose any position, be it a member of a board or advisory committee or a paid consultant, that they have been involved with that is related to this study. We also require that members of our journal advisory boards disclose their position when publishing in that journal. ***Please select one of the following:***

☒ We, the authors and our immediate family members, have no positions to declare and are not members of the journal's advisory board.

☐ The authors and/or their immediate family members have management/advisory or consulting relationships noted in the "declaration of interests" section of the manuscript and on this form below.

Patents

We require that you disclose any patents related to this work by any of the authors or their institutions. ***Please select one of the following:***

☐ We, the authors and our immediate family members, have no related patents to declare.

☒ We, the authors, have a patent related to this work, which is noted in the "declaration of interests" section of the manuscript and on this form below, and we have noted the patents of immediate family members.

Please insert any "declaration of interests" statements in this space. This exact text should also be included in the "declaration of interests" section of the manuscript. If no authors have a competing interest, please insert the text, "The authors declare no competing interests."

R. Tonelli and A. Pession are BIOGENERA shareholders. A.L. Scardovi, worked for BIOGENERA at the time of the studies, she is currently working for Ritrova Therapeutics, Inc. D. Bartolucci, S. Bortolotti, S. Angelucci, C. Amadesi, G. Nieddu, and L. Cerisoli are working at BIOGENERA. No potential conflicts of interest were disclosed by the other authors.

☒ **On behalf of all authors, I declare that I have disclosed all competing interests related to this work. If any exist, they have been included in the "declaration of interests" section of the manuscript.**